Hindawi
International Journal of Antennas and Propagation
Volume 2023, Article ID 5667834, 10 pages
https://doi.org/10.1155/2023/5667834

Research Article

An Ultra-Wideband MIMO Bowl-Shaped Monopole Antenna with Sturdy and Simple Construction

Changxian Li,[1] Pin Wen,[1] Xiujuan Lin,[2] Di Wu,[3] and Changfei Zhou [4,5]

[1]*National and Local Joint Engineering Research Center for Rail Transit Equipment, Dalian Jiaotong University, Dalian, China*
[2]*School of Information and Communication Engineering, Dalian University of Technology, Dalian, China*
[3]*College of Electronics and Information Engineering, Shenzhen University, Shenzhen, China*
[4]*School of Information and Communication Engineering, Dalian University of Technology, Dalian, China*
[5]*State Key Laboratory of Millimeter Waves, Southeast University, Nanjing, China*

Correspondence should be addressed to Changfei Zhou; cfzhou@dlut.edu.cn

Received 17 February 2023; Revised 28 June 2023; Accepted 17 July 2023; Published 29 July 2023

Academic Editor: Jun Xiao

Anultra-wideband (UWB) bowl-shaped monopole antenna with a sturdy, simple, and lightweight structure is proposed, and then is used to compose the 3 × 3 multiple input multiple output (MIMO) antenna. The wide bandwidth is determined by the outline of the monopole, which has a quarter wavelength and high-order modes. The inner part of the bowl-shaped monopole is removed for a light weight. The simulated and measured results show that an ultra-wide band of 2.3–8.1 GHz (5.8 GHz, 111.5%) and a high isolation of greater than 20 dB between the antenna elements of the MIMO antenna can be achieved.

1. Introduction

In modern vehicle-to-X (V2X) communication systems, vehicles are required to provide the in-car and out-car wireless information exchange for different systems, such as the train control and management system (TCMS), sub-6 GHz base station, and WiFi [1]. To support a higher transmission rate, the base station communication has developed from 2G to 5G, and the WiFi-6E band (5925–7125 MHz) has been introduced from the existing WLAN bands of 2400–2484 MHz and 5150–5925 MHz [2, 3]. Thus, an ultra-wideband (UWB) antenna backing up different frequency bands is preferred than the multiple antennas to save space and cost [4]. Since the vehicle is moving fast, the unavoidable vibration may cause the unreliable wireless link. To mitigate the effects of mobility and obtain an enhanced channel capacity, integrating the multiple input multiple output (MIMO) technique and omni-directional radiation performance with UWB can further facilitate the robustness of the communication system [5, 6]. For the terminal antenna, a sturdy, lightweight, and simple structure is also indispensable when the vehicle is moving fast.

With their wideband and omni-directional radiation properties, monopole antennas have been widely used to achieve UWB-MIMO antennas [7–13]. In [7], a top-hat monopole antenna was conceived to achieve a conical radiation pattern, but it had a narrow bandwidth. By introducing four metallic parasitic columns and a capacitive disk to a conical monopole, a 2.9 : 1 impedance bandwidth (IMBW) was obtained [8] with a complex structure. In [9], only a conical monopole antenna was designed to simplify the structure, but the weight was heavy due to the solid brass cone's high profile. Perforated alloy surfaces were adopted to realize lightweight structure in [10]. However, a 3D printing technique was required, resulting in a high cost. In [13], novel wideband roll-monopole antennas were devised, but the structures were not sturdy. Among the monopole antennas [7–13], the structures are either complicated or heavyweight. To achieve UWB-MIMO antennas, decoupling structures, such as ground stubs, defected ground slots, and reflectors, are mostly used to improve the isolation [14–18], which also complicates the design. Thus, designing an UWB-MIMO antenna with sturdy and simple construction is necessary for vehicle applications.

In this paper, a 3×3 MIMO antenna based on a UWB bowl-shaped monopole antenna is presented for vehicle applications. First, the bowl-shaped monopole with and without the inner part is studied for its light weight. The outline of the monopole is optimized to achieve a broad band with a sturdy structure. Then, the 3×3 MIMO antenna is made with a wide band and high isolation. Finally, the prototype is fabricated and measured for verification, showing a good radiation performance.

2. Antenna Design

2.1. Antenna Structure. The configuration of the proposed stepped monopole antenna element is depicted in Figure 1, with a simple and robust structure. The whole structure is like a bowl with an extended edge. The outline of the bowl antenna consists of a series of oblique lines to enhance the depth of the impedance matching. The coordinate system is established with the bottom point of the radiator as the coordinate origin. The antenna profile $z = f(x)$ equation is as follows:

$$f(x) = \begin{cases} x + 1 & 2 \le x < 3, \\ \frac{3}{2}x - \frac{5}{2} & 3 \le x < 5, \\ x & 5 \le x < 8, \\ \frac{2}{3}x + \frac{8}{3} & 8 \le x < 14, \\ \frac{5}{3}x - \frac{34}{3} & 14 \le x < 17, \\ 5x - 68 & 17 \le x < 18, \\ 22 & 18 \le x < 23, \\ 23 & 23 \le x \le 23.5. \end{cases} \tag{1}$$

Four nylon posts are placed between the bowl edge and the ground plane to support the structure's stability. The antenna is excited with the help of a SMA connector, with an extended inner pin inserting into the bottom of the bowl monopole. Finally, the antenna element is used to construct a 3×3 MIMO antenna, arranging it in line, as shown in Figure 2. The final optimized parameters are included in Table 1 for fabricating the prototype.

2.2. Antenna Analysis. To achieve a light weight, the inner part of the bowl-shaped monopole is removed. The reflection coefficients of the antenna with and without the inner part are compared in Figure 3, indicating that the inner part has no effect on the antenna performance. Thus, an empty bowl-shaped monopole is used to reduce the weight, exhibiting an impedance bandwidth of 2.3–8.1 GHz (5.8 GHz, 111.5%).

To further analyze the operating mechanism of the proposed antenna, current distributions at 2.4, 4, 6, and 7.5 GHz are presented in Figure 4. It can be seen that the current is mainly distributed outside the bowl monopole; thus, the inner part has little effect on the reflection coefficient. Since the currents are uniformly distributed along the same altitude, omni-directional radiation patterns can be acquired. The simulated results show that from 6.5 GHz to above, high-order mode can be observed from the current distribution, while the currents below 6.5 GHz exhibit a quarter wavelength along the monopole.

The outline of the bowl-shaped monopole dominantly affects the impedance matching. Two parameter studies are presented, for example, the reflection coefficients of different R_0 and R_7 are shown in Figure 5, affecting the higher and lower resonant frequencies, respectively. To have a wide bandwidth and good impedance matching, $R_0 = 2$ and $R_7 = 5$ mm are selected.

2.3. 3 × 3 MIMO Antenna. To increase the channel capacity, a 3×3 MIMO antenna is constructed based on the antenna element. To simplify the structure, three antennas are placed in line at a distance of 115 mm for high isolation. Finally, a cover box made of polycarbonate with a dielectric constant of 2.9, which can be combined with the ground by screws, is used to protect the MIMO antenna. Since this material has the property of fire prevention, the antenna inside is more practical for vehicle applications. The simulated reflection and transmission coefficients of the MIMO antenna with and without the cover are shown in Figure 6. It can be seen that the cover has little effect on the results of the reflection and transmission coefficients. Although a small variation in isolation can be observed, the overall isolation remains higher than 20 dB within 2.3–8.1 GHz. The IMBWs of the three antenna elements remain about 2.3–8.1 GHz, and the isolations are higher than 20 dB within the operating band.

The isolation with different values of interelement distance d is also investigated in Figure 7. It can be seen that when the three antenna elements are arranged in parallel, the isolation basically shows a downward trend with the increase in frequency. For WiFi/WLAN applications, the band of 2.4–2.4835 GHz is important; thus, the isolation between different antenna elements at 2.4 GHz should be kept larger. Considering the antenna fabrication tolerance and higher isolation, $d = 115$ mm is considered. When changing the ground width ub, the simulation found that s11, s22, and s33 did not change much, but the isolation s12 and s23 could not reach −20 dB, so $ub = 92$ mm is selected.

3. Simulated and Measured Results

The prototype of the proposed MIMO antenna is fabricated with a total dimension of $290 \times 92 \times 23.5\ \text{mm}^3$ ($2.22 \times 0.71 \times 0.18\ \lambda$, where λ is the free-space wavelength at the lowest frequency of 2.3 GHz), as shown in Figure 8. We use computer numerical control (CNC) to fabricate the antenna with aluminum, and 3D printing techniques are used to process the white cover plate. Finally, screws are

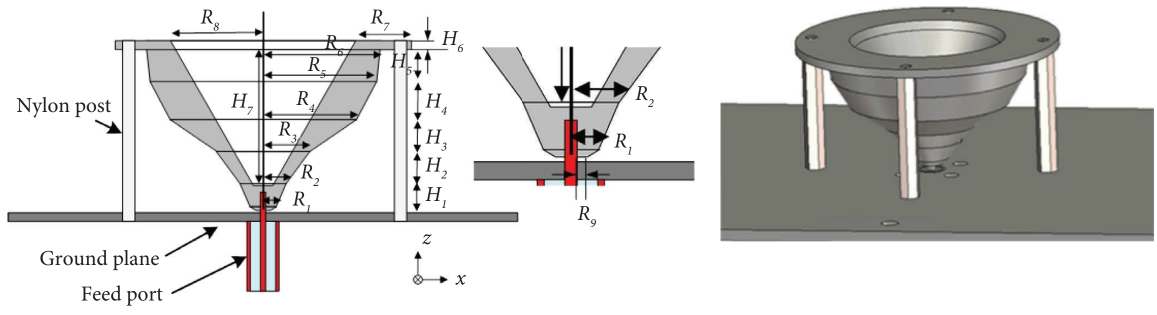

FIGURE 1: (a) Side view; (b) 3D view of the bowl monopole antenna.

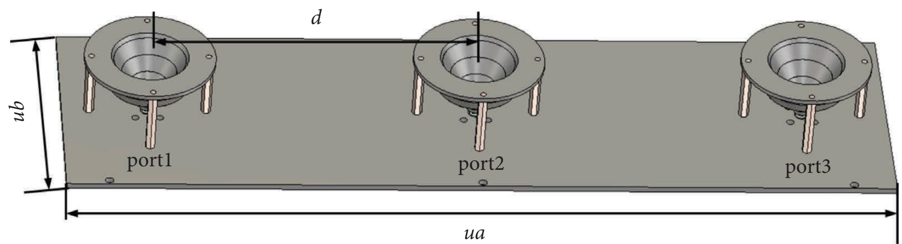

FIGURE 2: 3 × 3 MIMO antenna.

TABLE 1: Dimensions of the proposed antenna.

R_1	3
R_2	5
R_3	8
R_4	14
R_5	17
R_6	18
R_7	5
R_8	13.6
R_9	2
ub	92
H_1	4
H_2	3
H_3	4
H_4	5
H_5	6
H_6	1.5
H_7	19
d	115
ua	290

employed to assemble the antenna prototype and the white cover together. Considering the polycarbonate cover, the overall height of the antenna is 28 mm (0.21λ). The cover made of polycarbonate material is used to protect the MIMO antenna. Since this material has the characteristics of fire prevention, the antenna interior is more practical for vehicle applications. Compared with other works [9–12], whose structure is solid or requires several components, the proposed antenna, as a single component, is easy to fabricate by CNC, and the weight is light due to the hollow structure made of aluminum. Thus, the proposed antenna is more suitable for the use of vehicle antennas.

The reflection coefficients, isolation, and radiation patterns are measured. A comparison of the simulated and measured result of the *S*-parameters of the antenna is presented in Figure 9, showing a good agreement. The simulated IMBWs of the three antennas are in the range of 2.3–8.1 GHz, while the measured IMBWs are in the range of 2.3–9 GHz. Both the simulated and measured isolations are higher than 20 dB within 2.3–8.1 GHz. The discrepancy between the simulation and measurement can be accepted due to the fabrication and measurement errors.

The simulated and measured radiation patterns at different frequencies for port 1 and port 2 are shown in Figures 10–12 and Figures 13–15, respectively. Both copolarized (E-theta) and cross-polarized (E-phi) radiation patterns in the three principal planes are given. Since antenna 1 and antenna 3 have symmetrical positions, similar radiation patterns are achieved. Only the radiation patterns of antenna 1 and antenna 2 are shown in brief. A good agreement between the simulation and measurement is achieved. It can be seen that the *xoy* plane shows a consistent circular shape, and the *yoz* and *xoz* planes exhibit a doughnut shape with low cross-polarization, indicating a good omni-directional radiation performance.

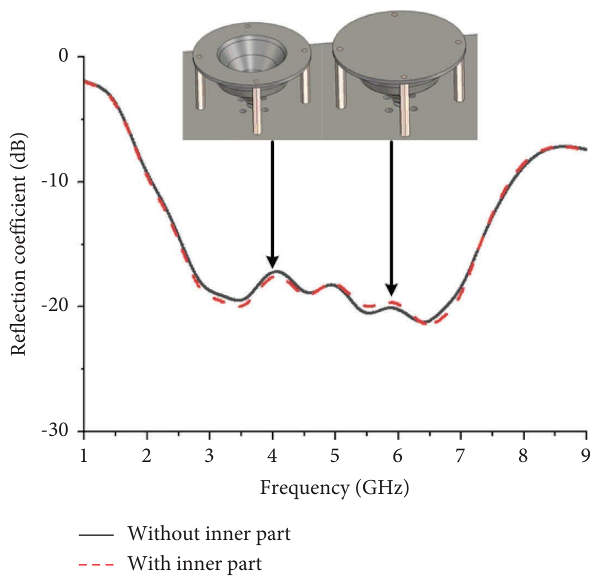

Figure 3: Reflection coefficient of the bowl antenna with and without the inner part.

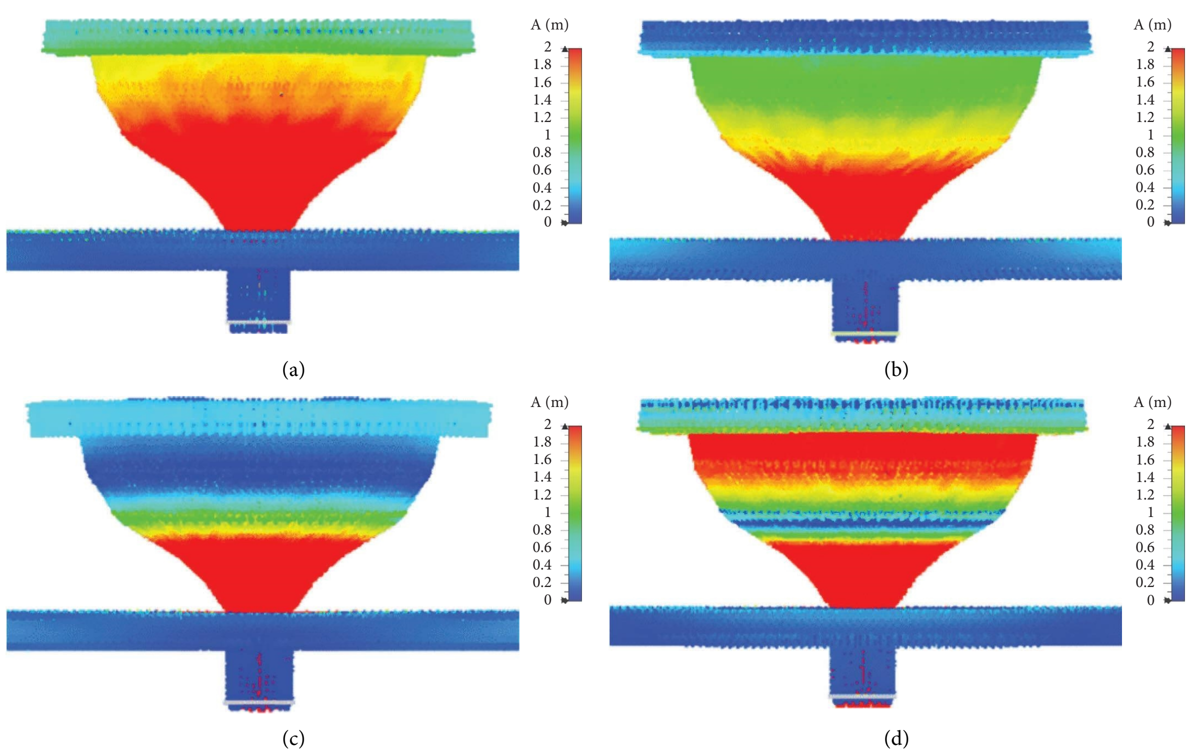

Figure 4: Current distributions at (a) 2.4 GHz, (b) 4 GHz, (c) 6 GHz, and (d) 7.5 GHz.

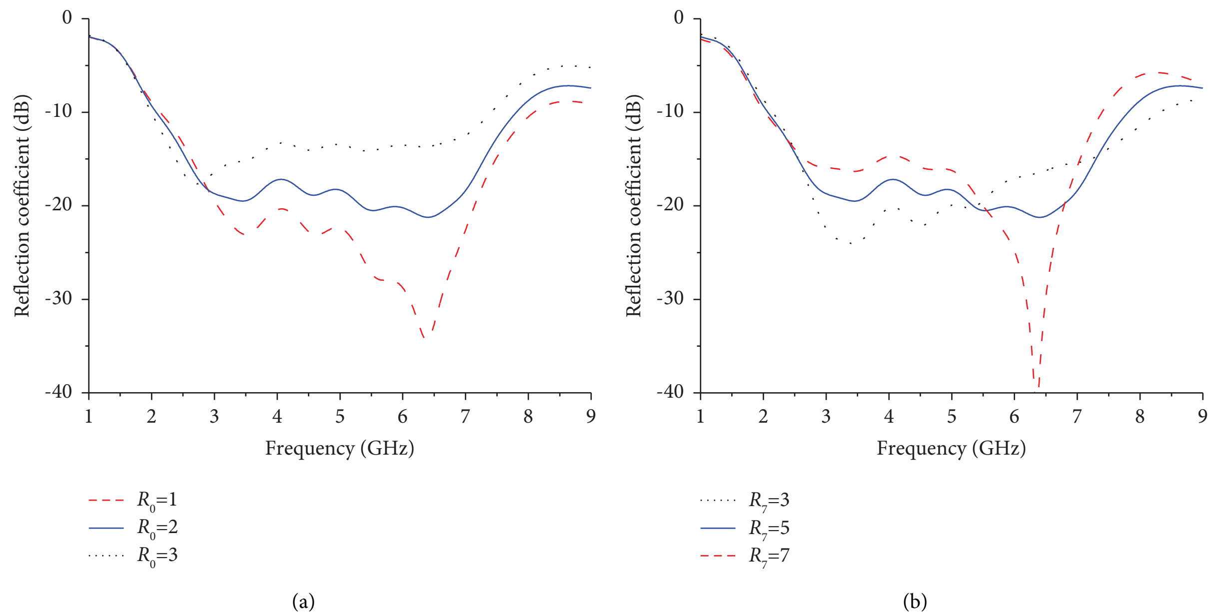

Figure 5: Reflection coefficients of different (a) R_0 and (b) R_7.

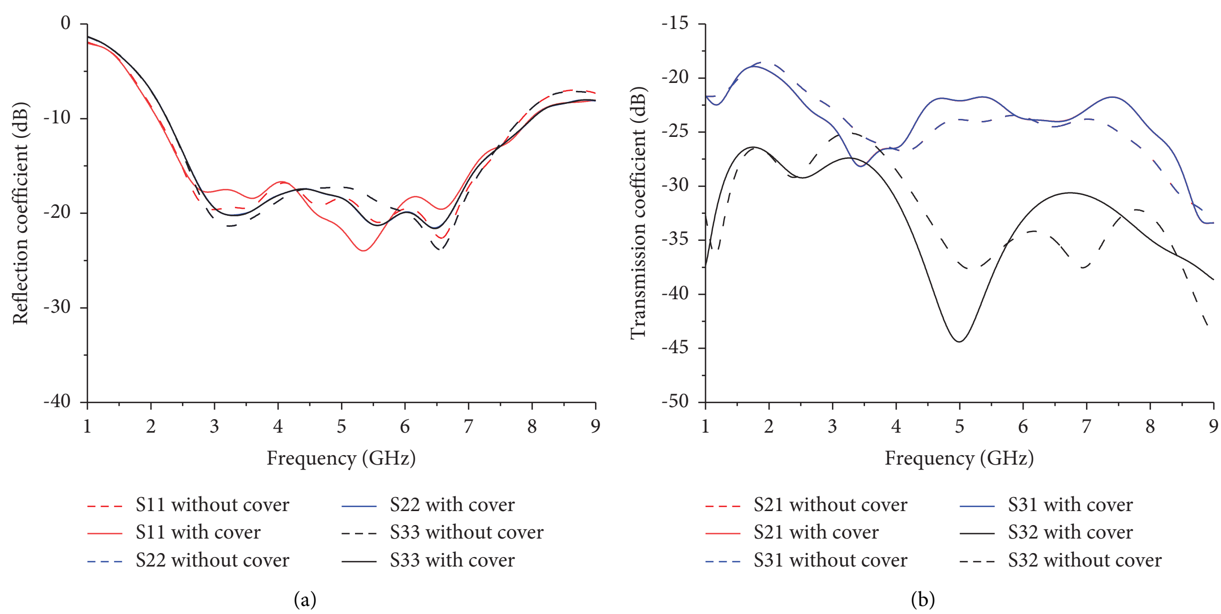

Figure 6: (a) Reflection and (b) transmission coefficients of the proposed antenna with and without cover.

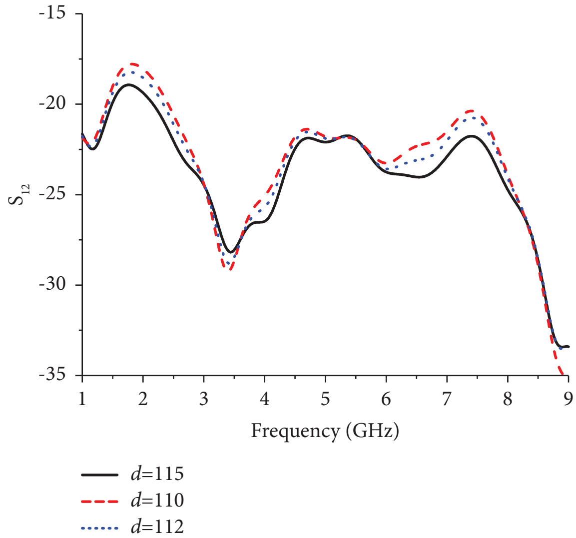

(a)

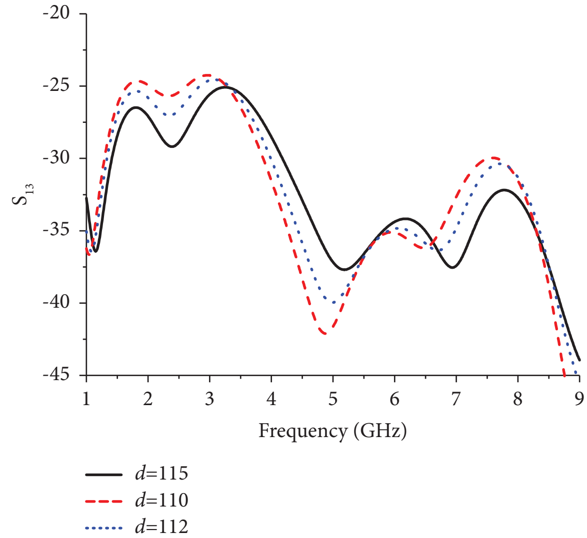

(b)

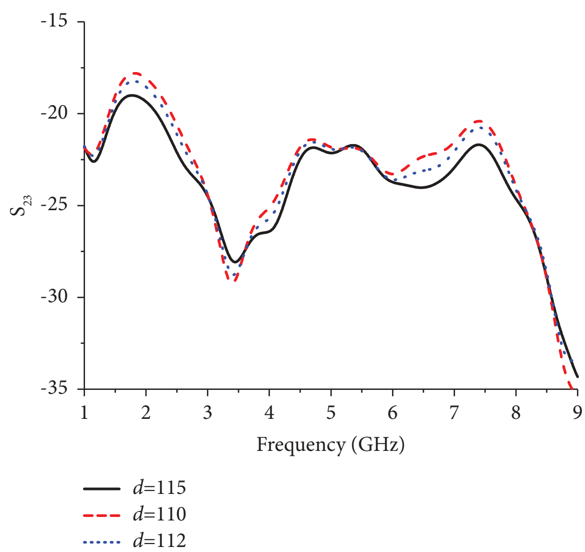

(c)

Figure 7: Effect of distance *d* variation on the isolation parameters (a) S12, (b) S13, and (c) S23.

(a)

(b)

Figure 8: The prototype of (a) the MIMO antenna and (b) polycarbonate cover.

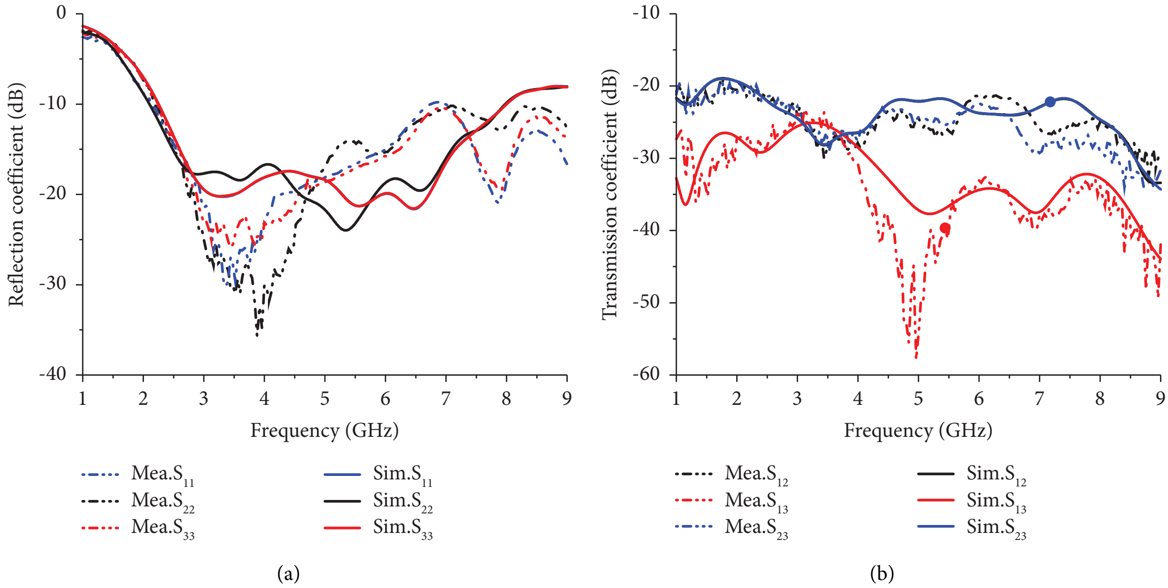

Figure 9: Simulated and measured (a) reflection and (b) transmission coefficients.

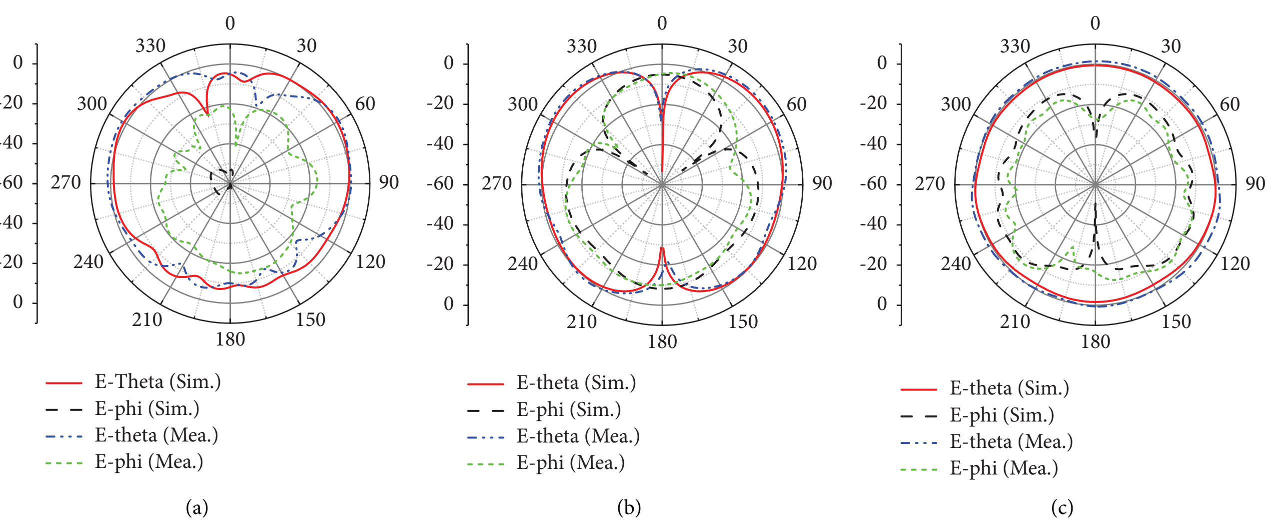

Figure 10: Simulated and measured radiation patterns for port 1 at 2.4 GHz in (a) *xoz*, (b) *yoz*, and (c) *xoy* planes.

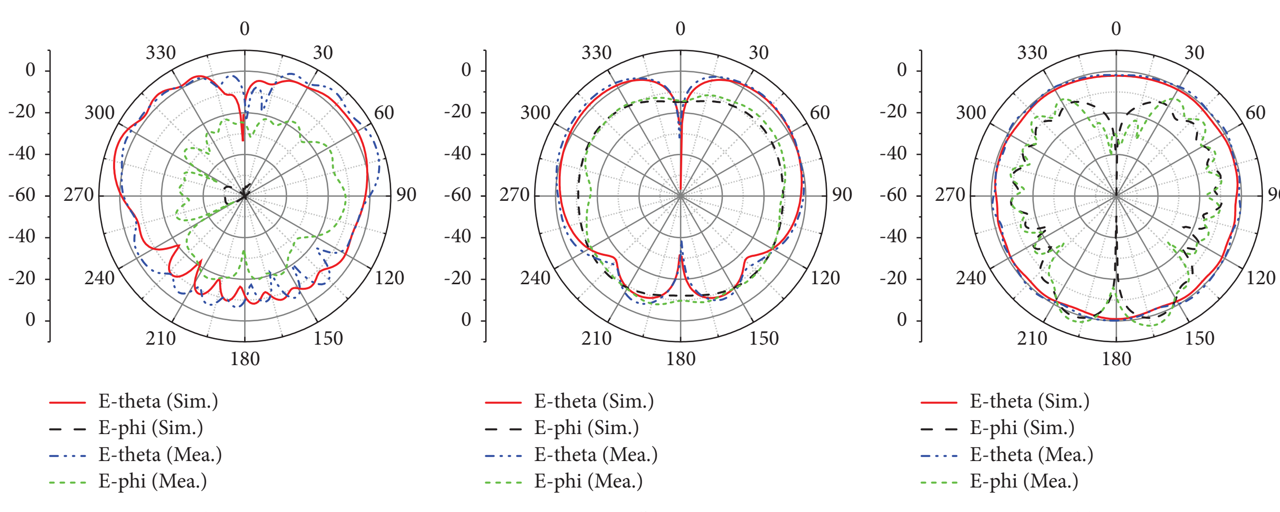

Figure 11: Simulated and measured radiation patterns for port 1 at 4 GHz in (a) *xoz*, (b) *yoz*, and (c) *xoy* planes.

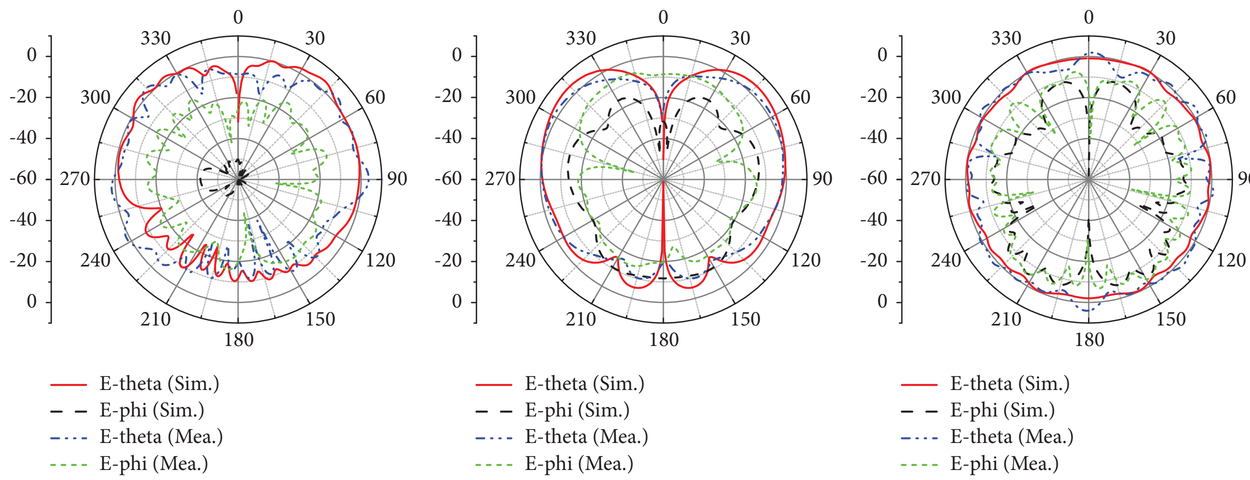

(a) (b) (c)

Figure 12: Simulated and measured radiation patterns for port 1 at 6 GHz in (a) *xoz*, (b) *yoz*, and (c) *xoy* planes.

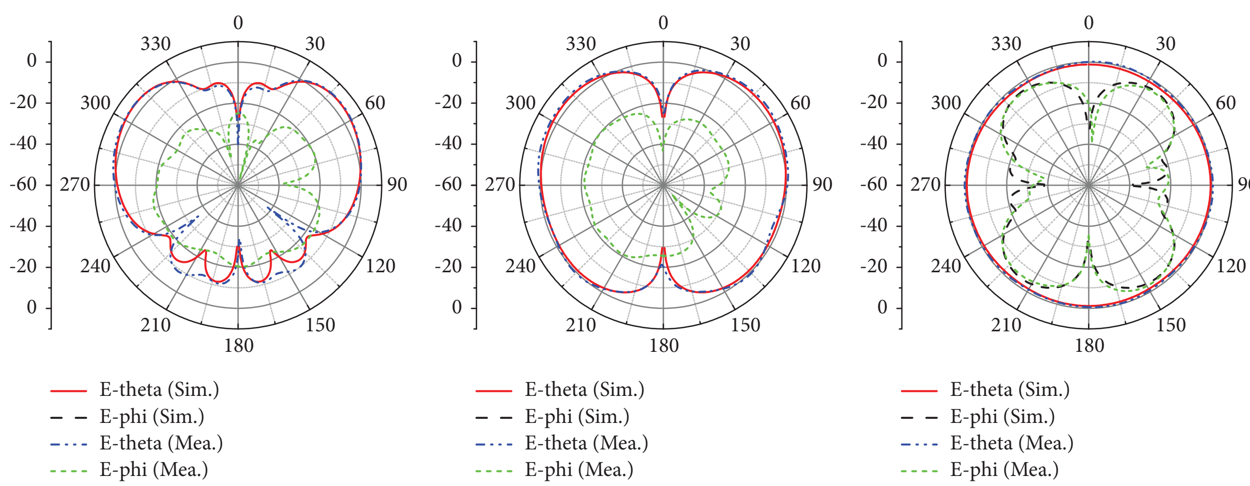

(a) (b) (c)

Figure 13: Simulated and measured radiation patterns for port 2 at 2.4 GHz in (a) *xoz*, (b) *yoz*, and (c) *xoy* planes.

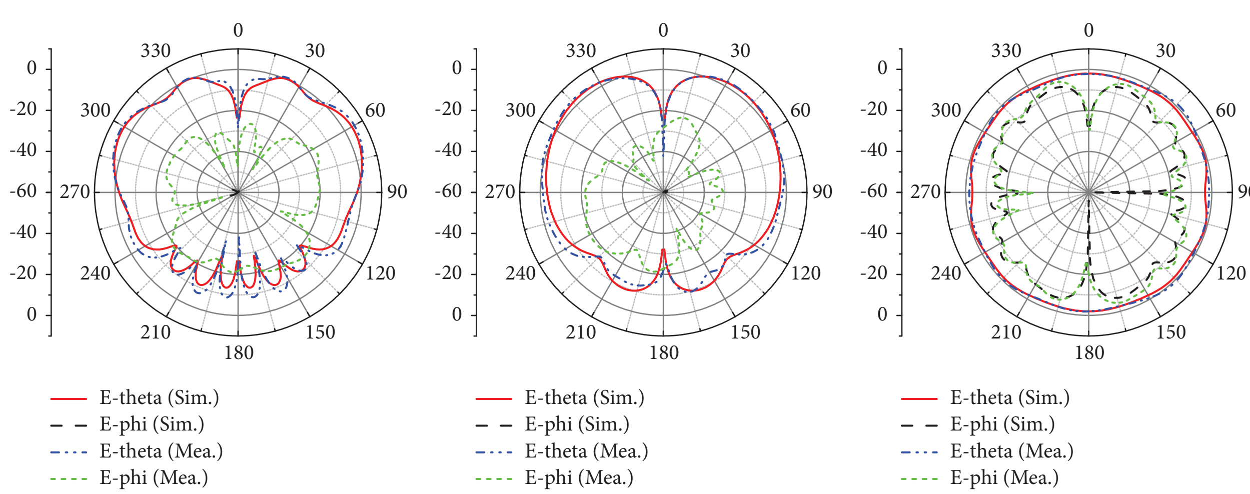

(a) (b) (c)

Figure 14: Simulated and measured radiation patterns for port 2 at 4 GHz in (a) *xoz*, (b) *yoz*, and (c) *xoy* planes.

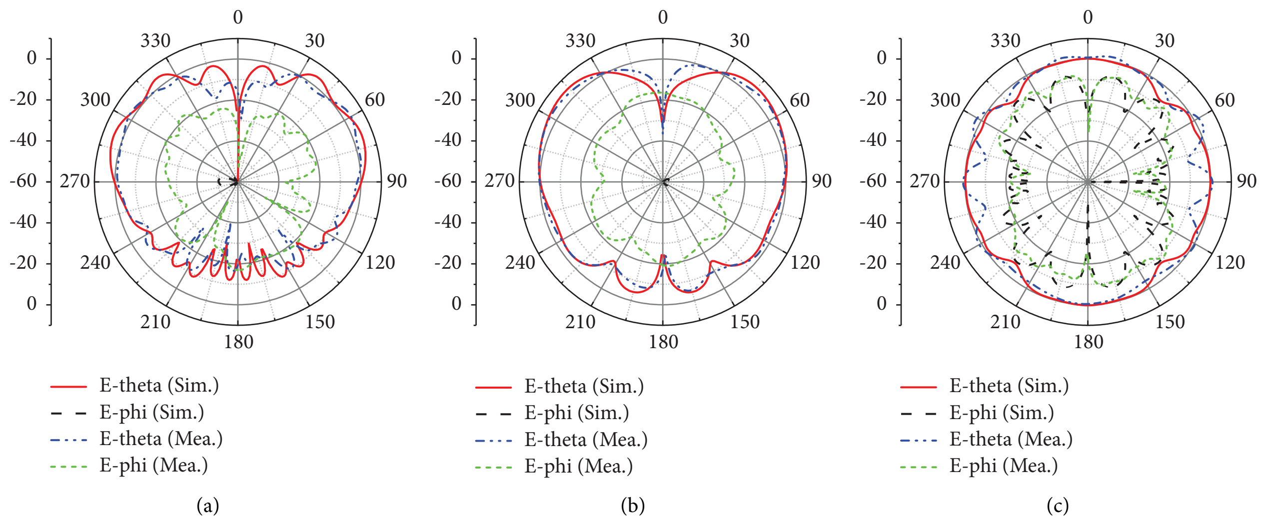

Figure 15: Simulated and measured radiation patterns for port 2 at 6 GHz in (a) *xoz*, (b) *yoz*, and (c) *xoy* planes.

4. Conclusions

The research on the 3 × 3 MIMO UWB monopole antenna has been designed and tested. A simple bowl-shaped monopole antenna with a sturdy structure is proposed for an ultra-wide band. A 3 × 3 MIMO antenna without any decoupling elements is constructed based on the bowl-shaped monopole, showing high isolation and wide bandwidths. A cover box made of fireproof material is used to protect the MIMO antenna, which has an insignificant impact on the antenna performance. The good performances and simple structure indicate the proposed antenna can be used for in-vehicle WiFi applications, covering 2400–2483.5 MHz, 5180–5825 MHz, and 5925–7125 MHz.

Data Availability

The data used to support the findings of this study are included within the article.

Conflicts of Interest

The authors declare that they have no conflicts of interest.

Authors' Contributions

CX Li developed the concept and supervised the whole project. P Wen and XJ Lin carried out the simulations. CF Zhou and CX Li analyzed the simulation data. P Wen and CF Zhou contributed to writing and finalizing the paper. XJ Lin and WD contributed to paper revision and language editing.

Acknowledgments

This work was supported in part by the Natural Science Foundation of China (Grant no. 62001080), China Postdoctoral Science Foundation (Grant no. 2022M712439), Fundamental Research Funds for the Central Universities (Grant no. DUT22JC32), and State Key Laboratory of Millimeter Waves Project (Grant no. K202319).

References

[1] B. Feng, B. Yang, C. Y. D. Sim, L. Deng, Z. Zhou, and X. Ding, "A compact vehicle-mounted garden-themed artistic antenna with isolation improvement for 2 G/3 G/LTE/5 G sub-6-GHz/WiFi/bluetooth communications," *IEEE Transactions on Vehicular Technology*, vol. 72, no. 4, pp. 4851–4862, 2023.

[2] C. Zhou, J. Sun, W. W. Yang, M. Li, and H. Wong, "A wideband low-profile dual-polarized hybrid antenna using two different modes," *IEEE Antennas and Wireless Propagation Letters*, vol. 22, no. 1, pp. 114–118, 2023.

[3] K. L. Wong, H. Y. Jiang, and W. Y. Li, "Decoupling hybrid metal walls and half-wavelength diagonal open-slots based four-port square patch antenna with high port isolation and low radiation correlation for 2.4/5/6 GHz WiFi-6E 4 × 4 MIMO access points," *IEEE Access*, vol. 10, pp. 81296–81308, 2022.

[4] M. G. N. Alsath and M. Kanagasabai, "Compact UWB monopole antenna for automotive communications," *IEEE Transactions on Antennas and Propagation*, vol. 63, no. 9, pp. 4204–4208, 2015.

[5] A. Al-Rawi, A. Hussain, J. Yang, M. Franzén, C. Orlenius, and A. A. Kishk, "A new compact wideband MIMO antenna—the double-sided tapered self-grounded monopole array," *IEEE Transactions on Antennas and Propagation*, vol. 62, no. 6, pp. 3365–3369, 2014.

[6] D. Potti, Y. Tusharika, M. G. N. Alsath et al., "A novel optically transparent UWB antenna for automotive MIMO communications," *IEEE Transactions on Antennas and Propagation*, vol. 69, no. 7, pp. 3821–3828, 2021.

[7] Z. Shen and J. Wang, "Top-hat monopole antenna for conical-beam radiation," *IEEE Antennas and Wireless Propagation Letters*, vol. 10, pp. 396–398, 2011.

[8] S. Palud, F. Colombel, M. Himdi, and C. Le Meins, "A novel broadband eighth-wave conical antenna," *IEEE Transactions on Antennas and Propagation*, vol. 56, no. 7, pp. 2112–2116, 2008.

[9] W. S. Yeoh and W. S. T. Rowe, "An UWB conical monopole antenna for multiservice wireless applications," *IEEE Antennas and Wireless Propagation Letters*, vol. 14, pp. 1085–1088, 2015.

[10] C. G. Hynes and R. G. Vaughan, "Conical monopole antenna with integrated tunable notch filters," *IEEE Antennas and Wireless Propagation Letters*, vol. 19, no. 12, pp. 2398–2402, 2020.
[11] P. A. Dzagbletey, J. Y. Jeong, and J. Y. Chung, "Ultra-wideband trident inset-fed monopole antenna with a 3-D conical ground," *IEEE Access*, vol. 9, pp. 2592–2601, 2021.
[12] D. Yang, J. Hu, and S. Liu, "A low profile UWB antenna for WBAN applications," *IEEE Access*, vol. 6, pp. 25214–25219, 2018.
[13] Z. N. Chen, "Broadband roll monopole," *IEEE Transactions on Antennas and Propagation*, vol. 51, no. 11, pp. 3175–3177, 2003.
[14] J. Ren, W. Hu, Y. Yin, and R. Fan, "Compact printed MIMO antenna for UWB applications," *IEEE Antennas and Wireless Propagation Letters*, vol. 13, pp. 1517–1520, 2014.
[15] C.-M. Luo, J.-S. Hong, and L.-L. Zhong, "Isolation enhancement of a very compact UWB-MIMO slot antenna with two defected ground structures," *IEEE Antennas and Wireless Propagation Letters*, vol. 14, pp. 1766–1769, 2015.
[16] M. H. Wang, J. C. Nan, and J. Liu, "High-isolation UWB MIMO antenna with multiple X-shaped stubs loaded between ground planes," *International Journal of Antennas and Propagation*, vol. 2021, Article ID 1155471, 13 pages, 2021.
[17] A. Mchbal, N. Amar Touhami, H. Elftouh, and A. Dkiouak, "Mutual coupling reduction using a protruded ground branch structure in a compact UWB owl-shaped MIMO antenna," *International Journal of Antennas and Propagation*, vol. 2018, Article ID 4598527, 10 pages, 2018.
[18] S. Zhang and G. F. Pedersen, "Mutual coupling reduction for UWB MIMO antennas with a wideband neutralization line," *IEEE Antennas and Wireless Propagation Letters*, vol. 15, pp. 166–169, 2016.